


Review

Catalysis inside Supramolecular Capsules: Recent Developments

Andrea Pappalardo ^{1,2}, Roberta Puglisi ¹ and Giuseppe Trusso Sfrassetto ^{1,2,*} 

¹ Department of Chemical Sciences, University of Catania, Viale A. Doria 6, 95100 Catania, Italy

² Department of Chemical Sciences, University of Catania Research Unit (I.N.S.T.M.) UdR of Catania, Viale A. Doria 6, 95125 Catania, Italy

* Correspondence: giuseppe.trusso@unict.it; Tel.: +39-0957385201

Received: 5 July 2019; Accepted: 19 July 2019; Published: 23 July 2019



Abstract: In the last decades, supramolecular chemists have developed new molecular receptors able to include a wide range of guests. In addition, they have designed synthetic hosts able to form capsules having an internal volume of thousands of Å³. This inner space shows different features from the bulk solution. In particular, this environment has recently been employed to perform chemical reactions, obtaining reaction products different from the “normal” conditions. These supramolecular capsules act as nanoreactors, catalyzing many chemical transformations. This review collects the recent developments (since 2015) in this field, focusing on supramolecular capsules based on resorcinarene hexameric capsules and metal-cage capsules.

Keywords: supramolecular catalysis; noncovalent capsule; resorcinarenes; cavitand; metal capsule

1. Introduction

Supramolecular catalysis in confined space is today a consolidated branched of the supramolecular chemistry, which is inspired by nature, in particular by natural enzymes. The goal of this approach is to create a micro- or nano-environment having features different from the bulk solution. In this confined space, reactivity is different with respect to the normal conditions in solution, and thus the rate of the reaction, as well as the products, can be different with respect to classic catalysis.

Enzymes provide a pocket (the active site) able to recognize the specific substrate via multiple interactions (such as hydrophobic interactions, hydrogen bonds, Lewis acid–base interactions), increasing the reaction rate, leading to stereo- and regioselective reactions. The modern supramolecular catalysts take inspiration from nature, designing artificial nanozymes able to include and transform specific substrates into the desired products.

A crucial point of the supramolecular catalysis in confined space is the proximity effect: reagents, hosted in a supramolecular capsule, are forced to be close to each other, removing the solvent molecules and thus leading to an increase of the activity/reactivity. In addition, the inclusion into a restricted space leads the reagent molecules to react each other with specific geometric constraints, leading to reaction products with regio- and stereoselectivity different from the normal conditions in solution.

A fundamental step in order to create an efficient supramolecular nanocatalyst is the design of the supramolecular host. Today, supramolecular chemistry offers many synthetic macrocycles which can be used to create a confined nanospace: resorcinarenes [1,2], cavitands [2–6], metallocages [7], and capsules assembled by hydrophobic interactions [8]. Although different supramolecular assemblies based on the abovementioned hosts have been studied for molecular recognition, regarding catalysis, only supramolecular containers assembled via hydrogen bonding and metal coordination have been reported to date. In fact, the use of oligomeric hosts such as cucurbiturils, cyclodextrins, crown ethers,

calixarenes, and carcerands is complicated due to their relatively small cavity dimensions and difficulty in obtaining larger receptors.

In 2015, a comprehensive review reported the applications of some nanocontainers in the catalytic field [9]. Thus, this review is focused on the recent catalytic applications to date since 2015.

2. Catalysis into Resorcinarene Hexameric Capsules

Resorcin[4]arenes are synthetic organic compounds able to form a hemispherical structure with a diameter of ca. 10 Å at the upper rim and a hydrophobic cavity with an internal volume of 350 Å³ that can accommodate many organic molecules [10]. These macrocycles are synthesized starting from resorcinol or 1,2,3-trihydroxyphenol and an appropriate aldehyde, which addresses the chemical characteristics of the lower rim [11]. The presence of eight hydroxyl groups on the upper rim opens the possibility of a wide functionalization range and of building supramolecular capsules exploiting hydrogen bonds [12].

By forming multiple hydrogen bonds, resorcin[4]arene **1** can form hexameric capsules through a self-assembly process first reported by Atwood and coworkers in 1997 (Figure 1) [13,14].

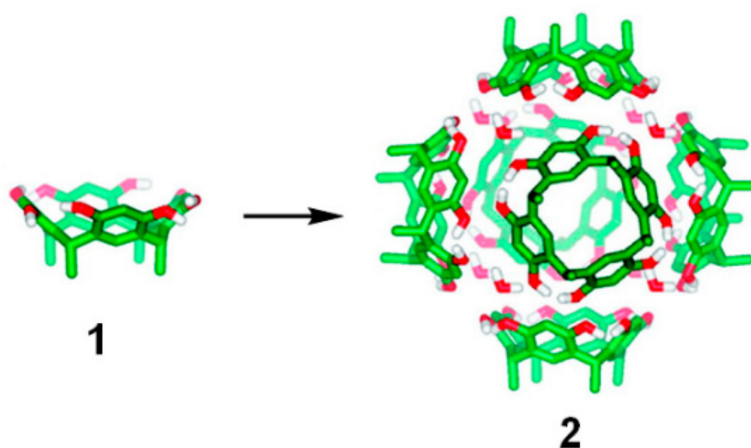
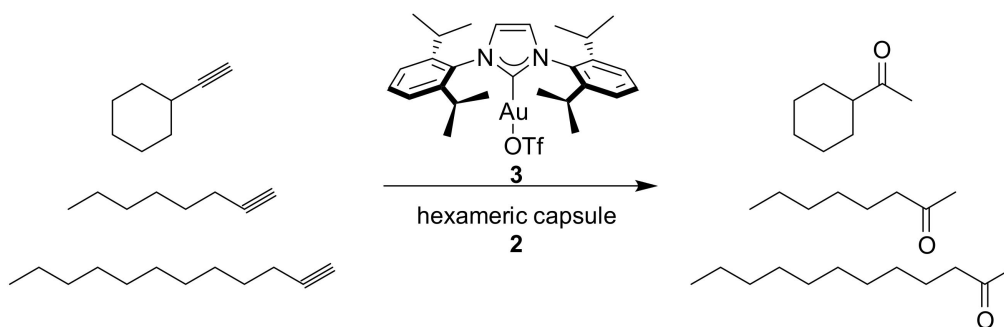


Figure 1. Resorcin[4]arene **1** and resulting hexameric capsule **2** (Adapted with permission from J. Am. Chem. Soc. 2008, 130, 2344. Copyright 2008 American Chemical Society).

The presence of water molecules is essential to the formation of the supramolecular assembly [15], which reaches an internal volume of ca. 1400 Å³, ideal for many organic reactions to be carried out inside. Assembly and molecular recognition properties of hexameric capsule **2** have been extensively investigated in solution [16–18]. A comprehensive review collected catalytic applications of resorcinarene capsules until 2014 [8]; in addition, a recent review by Gaeta and coworkers analyzed some important issues of the catalysis into capsule **2**, such as substrate selectivity, transition state stabilization, and acid- and hydrogen-bond-catalyzed reactions [19]. Furthermore, recently, cyclization reactions inside hexameric capsules have been summarized by Rebek [20]; thus, here, we have summarized the other recent developments.

The research group of Prof. Scarso has made a considerable contribution in this field. They reported the use of capsule **2** in the hydration reaction of alkynes [21]. In particular, they studied the effect of encapsulation of the gold catalyst **3** into **2** on substrate selectivity in the hydration of terminal alkynes (Scheme 1). The substrates tested differ structurally at a region far from the reactive triple bond.



Scheme 1. Hydration of terminal alkynes catalyzed by catalyst **3** included into capsule **2**.

Ethynylcyclohexane, 1-octyne, and 1-dodecyne were tested at 40 °C with 5 mol % of catalyst with and without the capsule. Reactions inside **2** are slower with respect to the free solution, due to the inclusion of the substrates inside the hydrophobic cavity. The reaction profiles showed in Figure 2 suggest a preference for the cyclic alkyne with respect to the linear one. In particular, the initial rate with ethynylcyclohexane is about three times higher than that obtained with linear substrates, while in the absence of the supramolecular capsule, the reaction rates are similar.

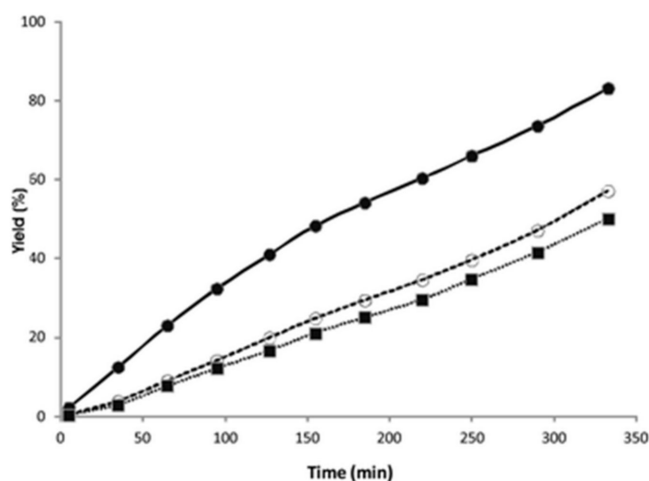


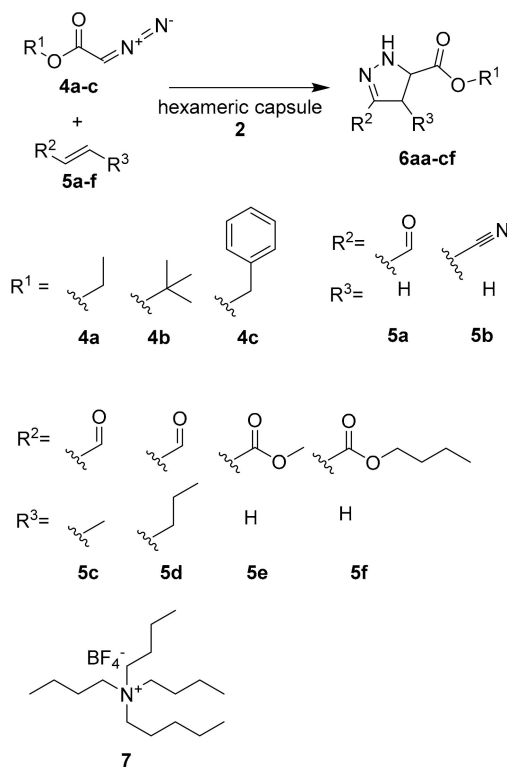
Figure 2. Competitive substrate selective hydration of ethynylcyclohexane (●), 1-octyne (○), and 1-dodecyne (■) catalyzed by **3@2** in water-saturated benzene- d_6 at 40 °C. (Reproduced from Ref. [21] with permission from The Royal Society of Chemistry.)

A possible explanation could be the different shape of the cyclic substrate compared to the linear ones. Then, the authors tested cyclic alkynes with different steric dimensions. Inside the capsule, the smaller aromatic alkyne reacted much faster than those of the bigger substrates, while in free solution, the reactivity is the opposite.

The same research group employed hexameric capsule **2** as the reactor for a dipolar cycloaddition reaction between diazoacetate esters and electron-poor alkenes (Scheme 2) [22].

The reaction occurs spontaneously at high concentration levels or can be catalyzed by Lewis acids/bases. When using acrolein as an active electron-poor alkene, the capsule leads to an increase of the yield respect to the free solution reaction (from 12% without capsule to 47% in the presence of the capsule) (see Table 1, entries 1 and 2). The addition of a large excess of tetrabutylammonium strongly decreases the yield, due to the inclusion of the cation in the cavity (Table 1, entry 3). In fact, tetrabutylammonium has a higher affinity for the cavity with respect to the reagents. The same trend is observed also with the other substrates, demonstrating that the dipolar cycloaddition reactions occur within the cavity with higher performance compared to in the absence of the supramolecular capsule.

Furthermore, the authors extended the screening of substrates to other electron-poor alkenes such as *trans*-crotonaldehyde and *trans*-2-hexenal. Very interesting are the cases of **5c–e** as substrates: in the absence of a capsule, no reaction occurs, while the presence of capsule **2** leads to a 95% of **5c** and 79% yield of **5d–e**. Using bigger substrates, the catalytic activity of the capsule decreases due to the steric hindrance.

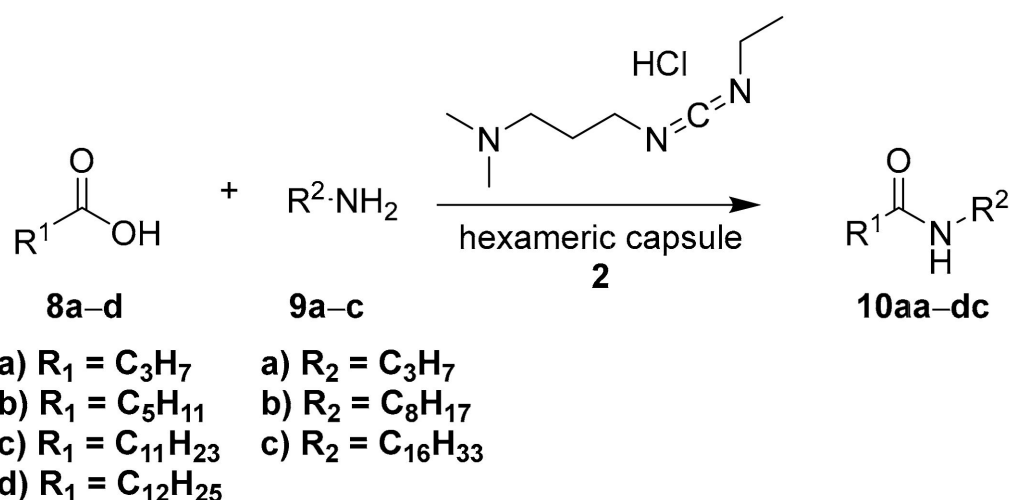


Scheme 2. Dipolar cycloaddition reaction catalyzed into hexameric capsule **2**; chemical structure of diazoacetate substrates; electron-poor alkenes; and competitive guest tetraethylammonium tetrafluoroborate.

Table 1. Catalytic tests for the 1,3-dipolar cycloaddition of diazoacetate esters with acrolein mediated by capsule **2**.

Entry	Diazoacetate	Capsule 2	Competitive guest 7	Product (Yield)
1	4a	No	No	6aa (12%)
2	4a	Yes	No	6aa (47%)
3	4a	Yes	Yes	6aa (8%)
4	4b	No	No	4ba (25%)
5	4b	Yes	No	4ba (97%)
6	4b	Yes	Yes	4ba (6%)
7	4c	No	No	4ca (18%)
8	4c	Yes	No	4ca (54%)
9	4c	Yes	Yes	4ca (5%)

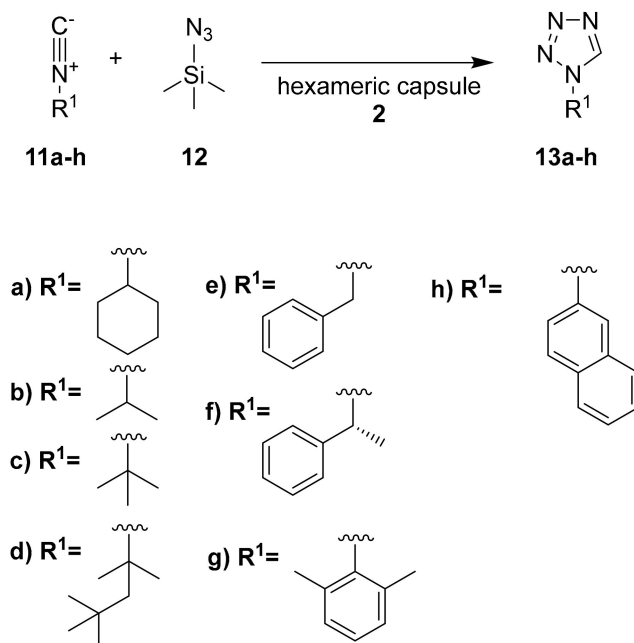
The synthesis of amides driven by a carbodiimide condensing agent is a reaction extremely widespread in organic chemistry. Scarso and coworkers used molecular capsule **2** as the nanoreactor for the synthesis of amides, starting from linear carboxylic acids and primary amines, by using *N*-(3-dimethylaminopropyl)-*N'*-ethylcarbodiimide hydrochloride (EDAC) as the activating agent (Scheme 3) [23].



Scheme 3. Amide 10 synthesis by coupling the reaction between carboxylic acids 8 and primary amines 9, mediated by a carbodiimide (EDAC), in the presence of the self-assembled capsule 2. EDAC: *N*-(3-dimethylaminopropyl)-*N'*-ethylcarbodiimide hydrochloride.

The hexameric capsule prefers shorter substrates, leading to the formation of the shorter amides, while in the absence of the capsule, the reactivity of all substrates is the same. These data suggest that the driving force for the substrate selectivity is the molecular recognition of the reagents, tuned by the steric effect.

Similar considerations can be related to the synthesis of 1H tetrazoles carried out in capsule 2 (Scheme 4) [24].



Scheme 4. Synthesis of 1H tetrazoles and chemical structure of substrates tested.

Table 2 shows the effect of the hexameric capsule in the click reaction using substrate 11a. In particular, no reaction occurs in the absence of the capsule. On the contrary, the presence of 10% of capsule 2 leads to the formation of the desired compound in an almost quantitative yield. The authors also tested the effect of a Bronsted acid (acetic acid) and resorcinol (Table 2, entries 3 and 4, respectively) in the absence of the hexameric capsule. Bronsted acids, in fact, can catalyze the reaction

in normal conditions. However, the obtained yields are lower with respect to the reaction inside the hexameric capsule. As previously reported, the presence of a competitive guest (TEA) inhibits the reaction, leading to a decrease of the yield (Table 2, entry 5).

Table 2. Catalysis tests for 1H tetrazole **13a** synthesis by reaction of cyclohexyl isonitriles **11a** and **12**.

Entry	Capsule 2	TEA ^a	t (h)	Yield (%) of 13a
1	No	No	5	0
2	Yes	No	6.5	>98
3 ^b	No	Yes	6	2
4 ^c	No	Yes	6	10
5 ^d	Yes	Yes	6.5	33

^a TEA = tetraethylammonium tetrafluoroborate as a competitive guest; ^b [Acetic acid] = (1 equiv. with respect to capsule 2); ^c [Resorcinol] = 318 mM (24 equiv. with respect to capsule 2); ^d [TEA] = 133 mM (10 equiv. with respect to capsule 2).

The authors tested also other aliphatic and aromatic substrates (Table 3). In general, the presence of the free capsule leads to higher yields with respect to the occupied cavity (the presence of TEA decreases the yield values). Notably, for aromatic substrates (**11g** and **11h**), the inhibition of the catalytic activity by using TEA is emphasized.

Table 3. 1H tetrazoles **13b–h** synthesis mediated by hexameric capsule 2.

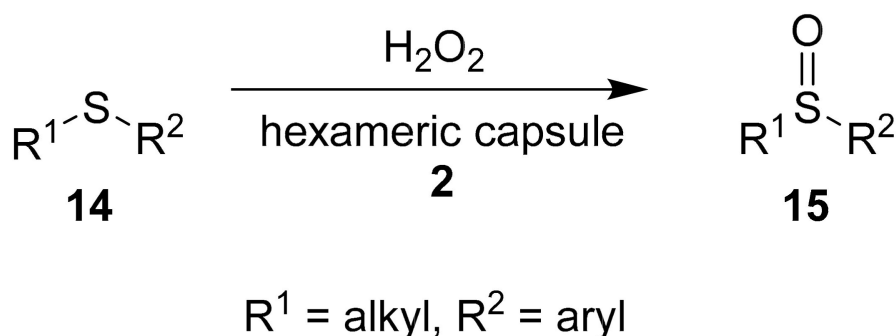
Entry	Substrate	Product	t (h)	Yield (%)
1	11b	13b	6.5	87 24 ^a
2	11c	13c	6	36 41 ^a
3	11d	13d	20	94 66 ^a
4	11e	13e	5.5	93 6 ^a
5	11f	13f	20	>98 19 ^a
6	11g	13g	6	40 2 ^a
7	11h	13h	6	81 4 ^a

^a In the presence of TEA (133 mM, 10 equiv. with respect to hexameric capsule 2).

Another important organic reaction catalyzed into hexameric capsule 2 is the sulfoxidation of thioethers, conducted under mild conditions within few hours (Scheme 5) [25].

The authors optimized the reaction using dibutyl sulfide as a substrate (Table 4). In particular, the positive effect of the hexameric capsule is demonstrated by the comparison of entries 1 and 2 in Table 4. In free solution, a yield of 10% is obtained after 90 min, while within the nano-environment, quantitative amounts of sulfoxide are obtained in 65 min. Due to the possibility of catalyzing the electrophilic oxidation of thioethers with H₂O₂ by the presence of phenols or acids, the authors tested the reaction with acetic acid and resorcinol (Table 4, entries 3 and 4, respectively). In both cases, although the yields are higher with respect to the uncatalyzed reaction (Table 4, entry 1), the efficiency of sulfoxidation is lower with respect to the encapsulated oxidation (Table 4, entry 2). Also, in this case, TEA was used as an inhibitor (Table 4, entries 5 and 6), leading to a moderate inhibition of the sulfoxidation. The authors assumed that the reaction is favored within the capsule due to the displacement of the water molecules

of hexameric capsule **2** by hydrogen peroxide, thus making it more electrophilic (oxidant activation). In addition, the transition state could be stabilized into the capsule by the electron-rich internal surface.



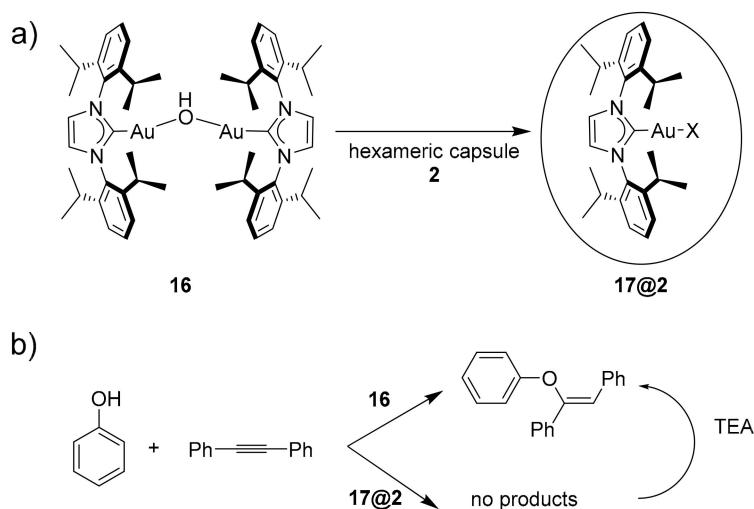
Scheme 5. Sulfoxidation of thioether **14** by using 30% H₂O₂, leading to sulfoxides **15** in the presence of hexameric capsule **2**.

Table 4. Catalytic tests for the sulfoxidation of dibutyl sulfide with 30% H₂O₂ ^a.

Entry	Capsule 2	TEA	t (min)	Yield (%)
1	No	No	90	10
2	Yes	No	65	>98
3 ^b	No	No	90	21
4 ^c	No	No	90	28
5	Yes	Yes	65	46
6	No	Yes	90	15

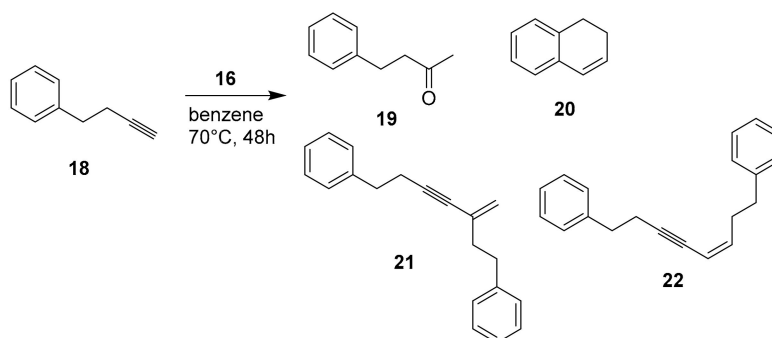
^a [**2**] = 36 mM, [**14**] = 60 mM, 30% H₂O₂ 1.2 equiv.; [TEA] = 60 mM. ^b [Acetic acid] = 6 mM (1 equiv. with respect to capsule **2**). ^c [Resorcinol] = 144 mM (24 equiv. with respect to capsule **2**).

Reek and coworkers exploited the ability of hexameric capsule **2** to inhibit or modify the reactivity of dimeric gold catalyst **16** (Scheme 6a) [26]. In particular, the dimeric catalyst **16** leads to the vinyl ether reported in Scheme 6b after 60 min in an almost quantitative yield. On the contrary, no products were observed after 24 h in the presence of the monomeric gold catalyst within the hexameric capsule **17@2**. The addition of TEA as a competitive guest regenerates the original dimeric gold catalyst, leading to the desired compound.



Scheme 6. (a) Encapsulation of gold dimeric catalyst **16**; (b) catalysis with dimeric catalyst **16** and monomeric encapsulated catalyst **17@2**.

Furthermore, the authors tested also the change of the reactivity in the presence of capsule **2**, using 4-phenyl-1-butyne **18** (Scheme 7).



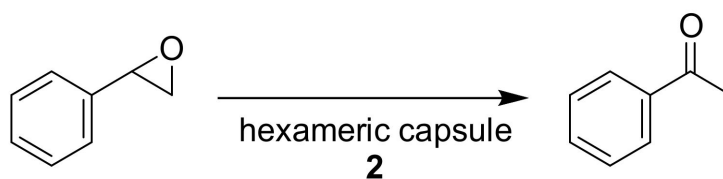
Scheme 7. Conversion of 4-phenyl-1-butyne **18**.

In the absence of the capsule, the catalyst can activate two molecules of alkyne, leading also to dimerization products **21** and **22** (Table 5, entry 1). The capsule favors the intramolecularly cyclized product **20** (Table 5, entry 2) due to the presence of mononuclear catalyst inside. The presence of the competitor (TEA) leads also to the dimerization products **21** and **22** (Table 5, entry 3).

Table 5. Gold-catalyzed conversion of 4-phenyl-1-butyne **18**.

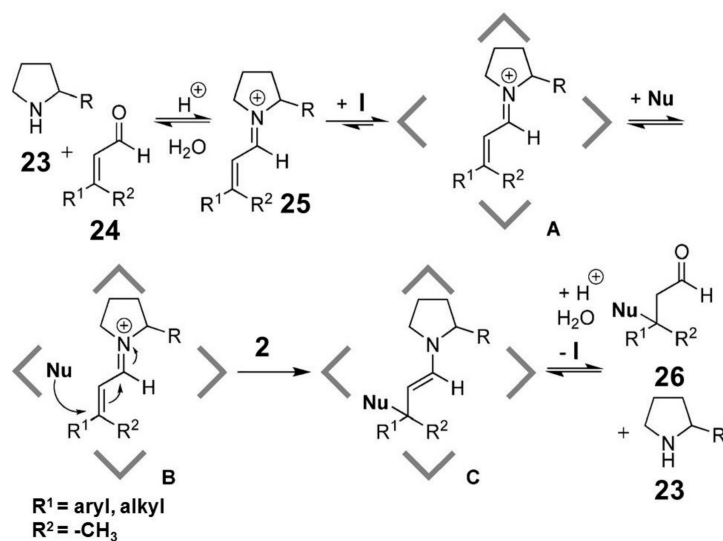
Entry	Capsule 2	TEA	Yield 19 (%)	Yield 20 (%)	Yield 21 (%)	Yield 22 (%)
1	No	No	7	0	38	8
2	Yes	No	3	16	0	0
3	Yes	Yes	47	0	28	4
4	No	Yes	6	0	47	8

The metal-free isomerization of epoxides into the corresponding carbonyl compounds in a hexameric capsule was also tested by Scarso and coworkers (Scheme 8) [27]. The reaction was optimized by using styrene oxide as a substrate. In the absence of the self-assembled capsule, no isomerization product was observed. Only the presence of capsule **2** in catalytic amounts (7%) led to the formation of phenylacetaldehyde in good yield after 3 h (69%), while a quantitative yield was achieved after 18 h. This is a clear example of how the inner space of a supramolecular capsule can act as an enzyme, catalyzing reactions which do not occur in free solution.



Scheme 8. Isomerization of epoxides inside capsule **2**.

Tiefenbacher and coworkers tested a hexameric capsule as the nanoreactor for enantioselective catalysis by using a chiral iminium organocatalyst (Scheme 9) [28]. Recognition properties of the supramolecular capsule towards cationic species were exploited in order to include the reactive iminium species **25** inside the hydrophobic cavity, leading to intermediate **A**. After the inclusion of the nucleophilic reagent (intermediate **B**), reaction occurs inside the nanoreactor, leading to the product **26** and reforming the starting catalyst **23**. By using chiral catalysts, the authors observed interesting results in term of enantiomeric excesses, observing reaction products with an *S*-configuration. The authors proposed that iminium cation **25** interacts with the aromatic walls of the capsule via cation- π interactions from the less hindered face, selectively exposing the other face to the nucleophile (Figure 3).



Scheme 9. Proposed pathway of the iminium-catalyzed reaction inside hexameric capsule **2** (Adapted from Ref. [28], with permission of John Wiley and Sons).

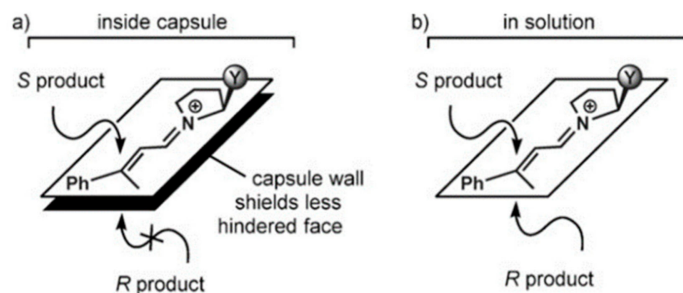
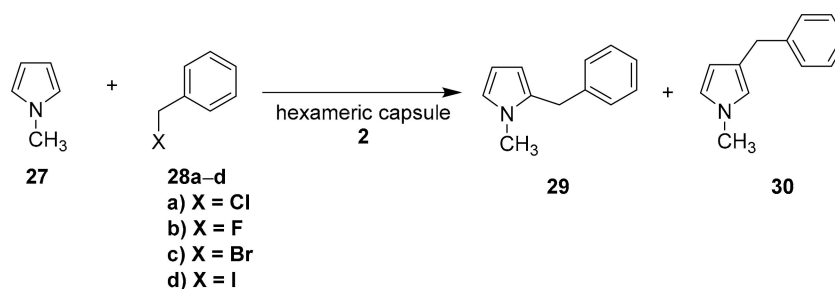


Figure 3. Hypothesis for the different selectivity inside capsule **2** (reproduced from Ref. [28], with permission of John Wiley and Sons).

Recently, Neri and coworkers reported the use of the capsule **2** to catalyze the Friedel–Crafts benzylation of several arenes and heteroarenes with benzyl chloride under mild conditions [29]. In particular, they tested the reaction between N-methylpyrrole **27** and benzyl halides (**28a–d**) in the presence of capsule **2** (Scheme 10).



Scheme 10. Friedel–Crafts reaction between N-methylpyrrole **27** and benzyl halides **28a–d** promoted by capsule **2** in water-saturated CDCl₃.

Reaction does not occur in the absence of the capsule (Table 6, entry 1). In addition, the product of β -alkylation (**30**) is favored in the presence of the capsule (Table 6, entry 2), although in normal conditions, the preferred product is **29** [30]. These data demonstrate how the inner space of the capsule can change reactivity. By increasing the amount of capsule and the temperature, yields and **30/29** ratio also increase (Table 6, entry 4).

Table 6. Optimization of Friedel–Crafts reaction.

Entry	Temp. (°C)	X	27 (Equation)	Capsule 2 (mol %)	Yield (%)	30/29
1	30	Cl	1.5	0	0	–
2	30	Cl	1.5	26	20	90/10
3 ^a	30	Cl	1.5	26	0	–
4	50	Cl	1.5	52	81	94/6
5	50	Br	1.5	52	72	91/9
6	50	F	1.5	52	75	85/15
7	50	I	1.5	52	–	–

^a In the presence of TEA.

The authors performed quantum-chemical studies in order to understand the preference of β -alkylation inside the capsule (Figure 4). In particular, some important pieces of evidence seem to justify the formation of **30**: (i) a hydrogen-bonding interaction between the chlorine atom and a bridging water molecule of the capsule; (ii) two different pKa values (2.5 and 6.1) of hydrogen atoms directly bonded to oxygen atoms in the capsule; (iii) the 1,2-benzyl shift.

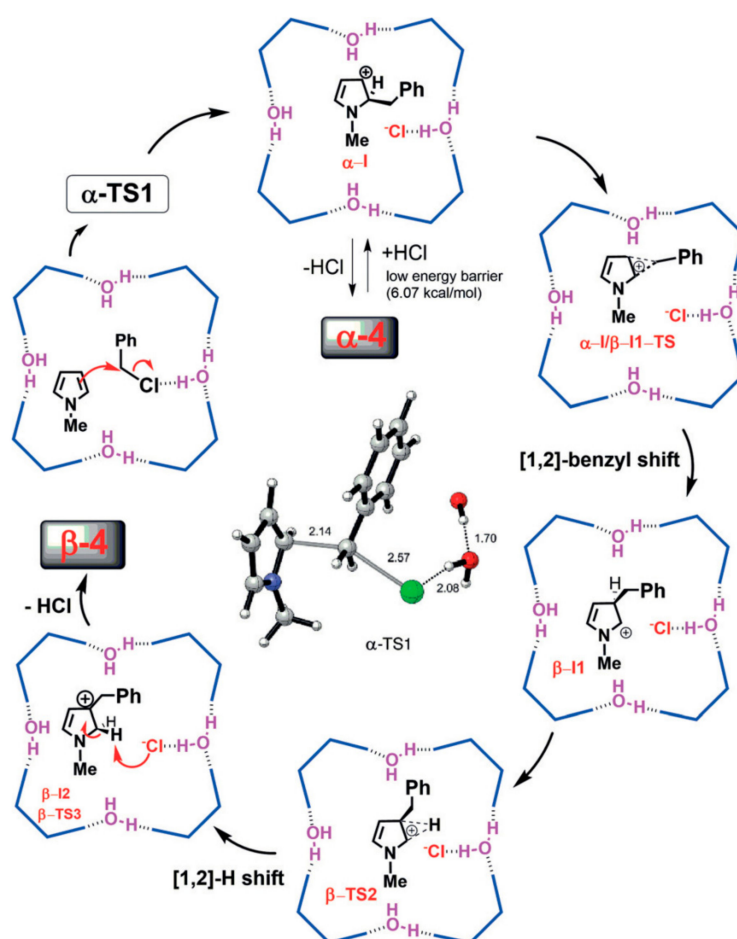


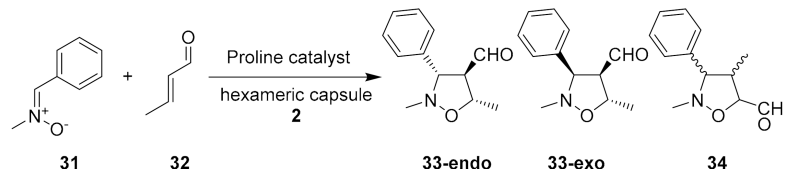
Figure 4. The mechanism proposed for the preferential formation of β -alkylation inside the capsule (Reproduced from Ref. [29], with permission of John Wiley and Sons).

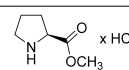
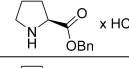
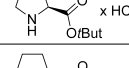
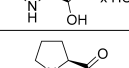
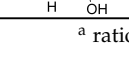
The same research group employed self-assembled capsule **2** to perform 1,3-dipolar cycloaddition [31]. In particular, they used nitrones and α , β -unsaturated aldehydes as substrates and *L*-proline derivatives as catalysts (Table 7). The presence of the capsule leads to a positive effect in the reaction. In all cases, in fact, the yields are higher with respect to the reaction conducted in the absence of the supramolecular cage. As reported in Table 7, capsule **2** also influenced the stereochemistry of the

reaction—in fact, the capsule leads to the formation of the **33-endo** diastereoisomer. On the contrary, in free solution, the diastereoisomer **33-exo** is favored. Furthermore, the enantioselectivity of the reaction is also strongly influenced by the hexameric capsule. Considering **33-endo**, in the presence of the capsule, the enantiomer *4R* is favored with respect to the *4S*, while the trend is the opposite in the absence of capsule **2**.

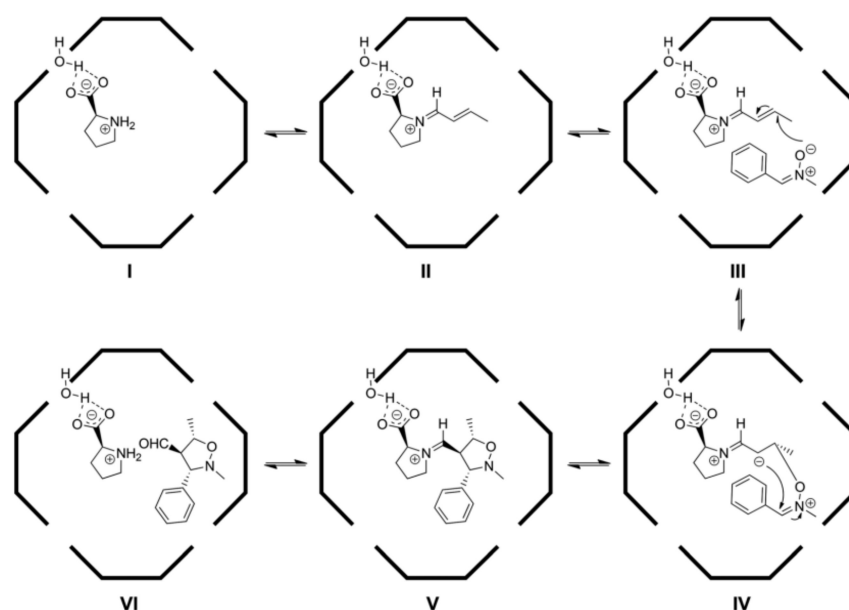
The authors performed a computer simulation to elucidate the mechanism involved (Scheme 11). They suggested that the hexameric capsule, after inclusion of reactants, acts as acid catalyst for the iminium condensation.

Table 7. Catalytic tests of cycloaddition between **31** and **32**.



Entry	Proline Catalyst	Capsule 2	Yield (%)	33-endo/33-exo/32 ^a	ee ^b 33-endo/33-exo
1	 x HCl	No Yes	42 88	24/67/9 86/1/13	14(4S)/7(3R) 43(4R)/–
2	 x HCl	No Yes	36 89	43/57/– 55/42/3	11(4S)/25(3R) 57(4R)/5(3R)
3	 x HCl	No Yes	– 44	– 24/67/9	– 1(4R)/–
4	 x HCl	No Yes	– 18	– 100/–/–	– 40(4R)/–
5		No Yes	– 90	– 84/14/2	– 95(4R)/8(3R)

^a ratio of concentrations of products; ^b ee = enantiomeric excess.



Scheme 11. Proposed mechanism of cycloaddition between **31** and **32** (reproduced from Ref. [31] with permission from The Royal Society of Chemistry).

3. Catalysis with Metallocape Capsules

Metal–ligand coordination shows an energy value of ca. 100–300 kJ/mol, and thus leads to the formation of a stable supramolecular capsule if the upper rim of a cavitand is functionalized with an appropriate chelating group able to bind a metal ion. After first pioneering study of Dalcanele and Jacopozi [32], many different metal-based supramolecular systems able to act as nanoreactors have been synthesized [8,9].

Recently, the research group of Prof. Reek synthesized a new tetragonal-prismatic nanocapsule, **35**, containing two Zn-porphyrins linked by four Pd-based macrocyclic walls able to include a chiral Rh catalyst for the regio- and enantioselective hydroformylation of styrenes (Figure 5) [33].

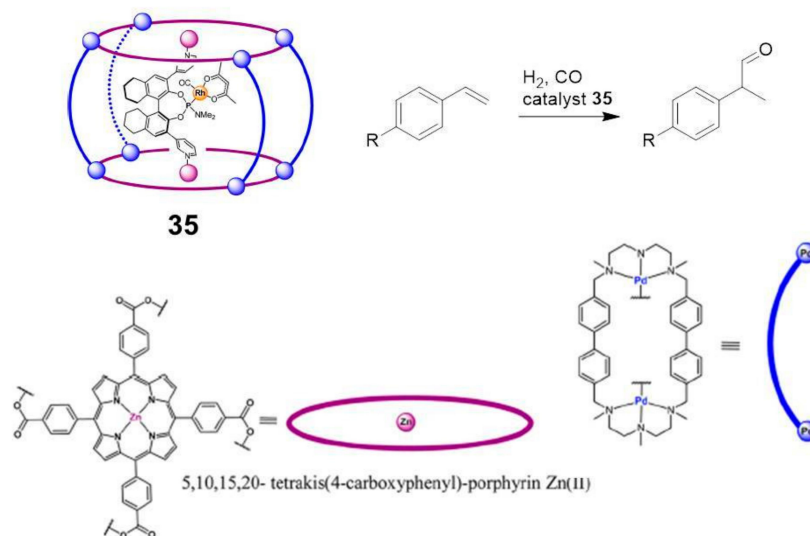


Figure 5. Representation of the capsule **35** containing Rh catalyst (adapted with permission from Ref. [33]. Copyright 2008 American Chemical Society) and hydroformylation of styrenes.

In particular, substrates differed with respect to the R-substituents on the para position of the aromatic ring. By comparison with results obtained in bulk solution, the stereoselectivity observed with the cage is higher, due to the role of a second coordination sphere of the Rh catalyst.

Raymond and coworkers reported the ability of a tetrahedral Ga-based capsule **36** (Figure 6) to photosensitize the 1,3-rearrangement of cinnamylammonium cations from the linear to the higher-energy branched isomer after UVA irradiation [34].

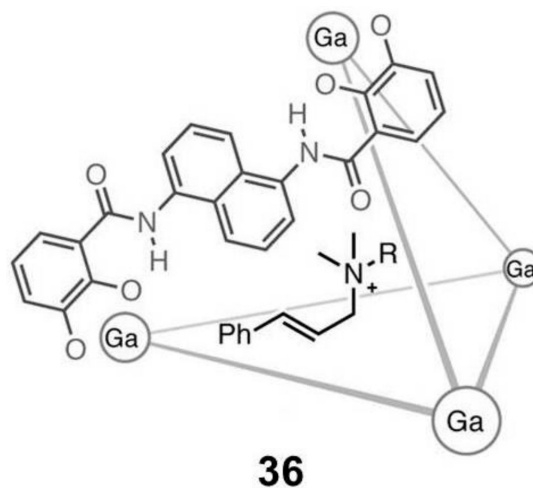
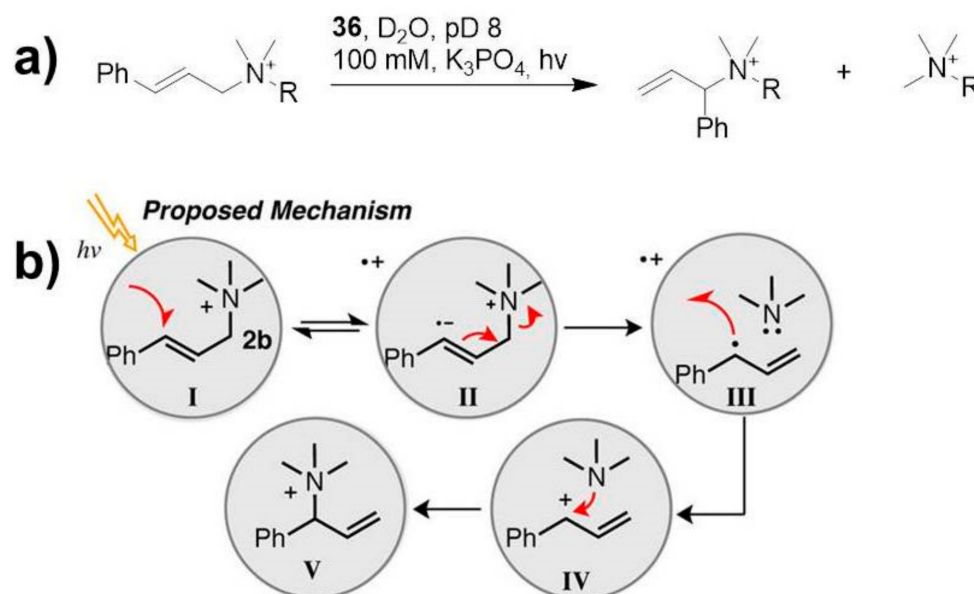


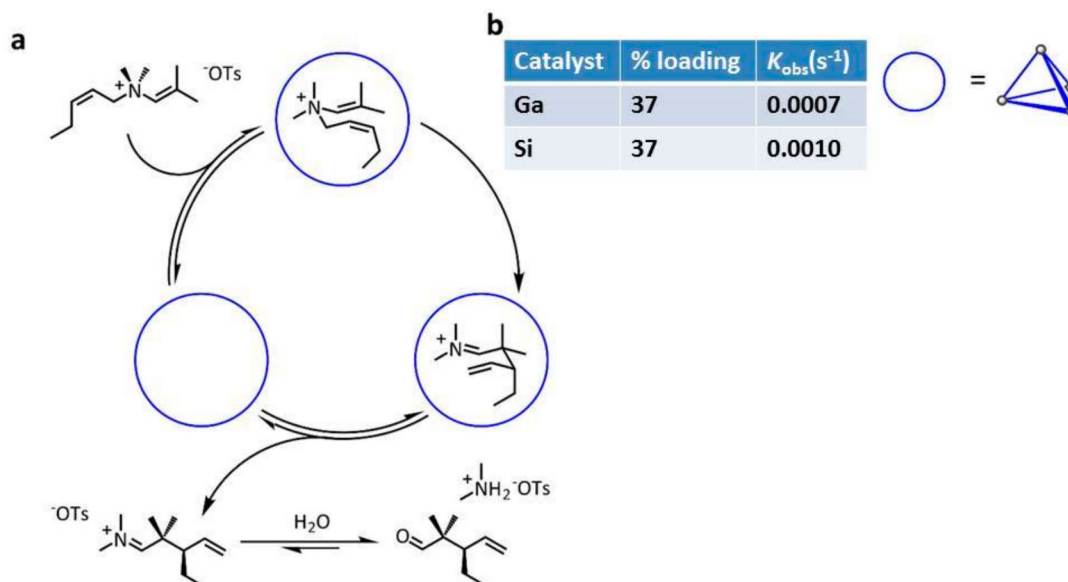
Figure 6. Ga-based tetrahedral capsule **36**.

In particular, cage **36** acts as a photosensitizer, transferring the energy to the included guest, leading to a rearrangement not observed in solution (Scheme 12).

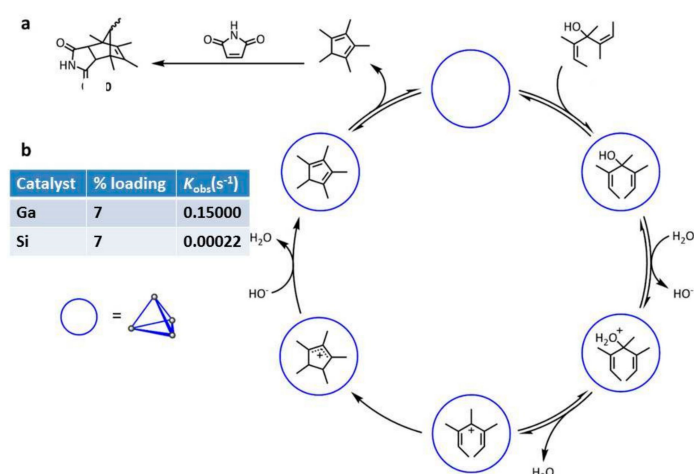


Scheme 12. (a) Rearrangement of cinnamylammonium cations inside cage **36**; (b) proposed mechanism (adapted with permission from Ref. [34]. Copyright 2008 American Chemical Society).

The same research group employed gadolinium capsule **36** and the analogue Si capsule in the aza-Cope rearrangement and in Nazarov cyclization (Schemes 13 and 14) [35].



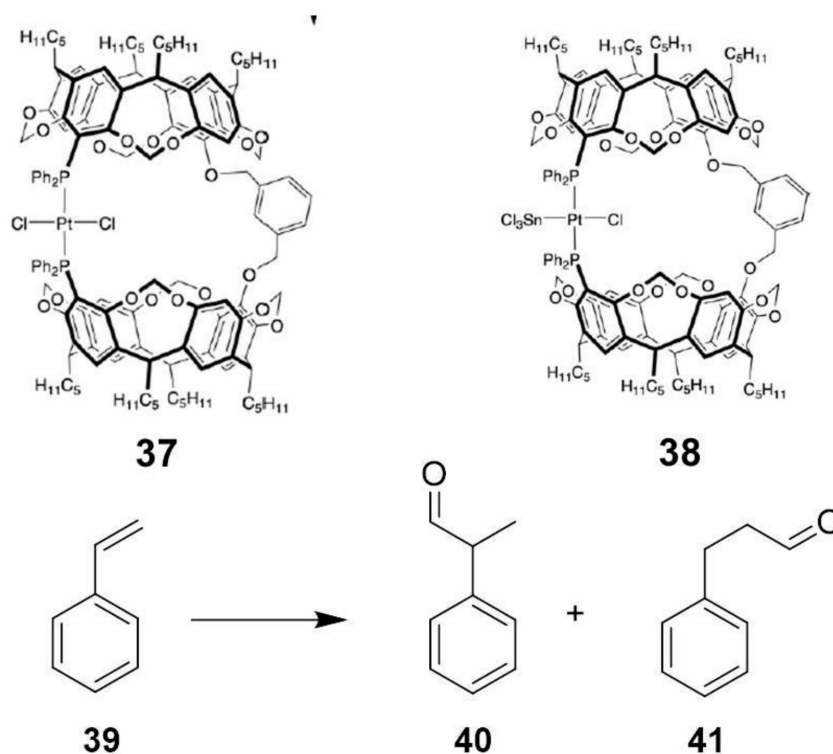
Scheme 13. (a) Proposed mechanism for Si- or Ga-catalyzed aza-Cope rearrangement. (b) Observed rate constants (k_{obs}) for the catalyzed aza-Cope rearrangement (adapted with permission from Ref. [35]. Copyright 2008 American Chemical Society).



Scheme 14. (a) Proposed mechanism for Si- or Ga-catalyzed Nazarov rearrangement. (b) Observed rate constants (k_{obs}) for the catalyzed Nazarov rearrangement (adapted with permission from Ref. [35]. Copyright 2008 American Chemical Society).

In particular, both metallocages show comparable catalytic activity for the aza-Cope rearrangement, while in the Nazarov rearrangement, a 680-fold increase of the reaction rate is observed. This is probably due to the increase of the charge of the starting neutral substrate, leading to cationic transition states stabilized by the anionic capsule.

The research group of Prof. Matt employed a resorcinarene platform to build a metallocage able to catalyze the hydroformylation of styrene (Scheme 15) [36]. Due to a hydrophobic cavity having a diameter of ca. 8 Å, resorcinarene hosts possess an ideal platform to create nanoreactors [37,38]. In particular, two resorcinarene cavities can be linked with a phenyl ring and a Pt ion, leading to nanocages 37 and 38 (Scheme 15).



Scheme 15. Nanocages 37 and 38 and hydroformylation of styrene.

Table 8 reports the results of the hydroformylation of styrene obtained by using metallocages 37 and 38. While the noncapsular catalyst leads to similar amounts of branched and linear products (40 and 41, respectively) in 24 h, the nanocages lead to the preferential linear aldehyde 41. Molecular modeling suggested that steric interactions between the guest and the capsule walls are slightly lower for the branched guest than for the linear one, thus explaining the observed selectivity.

Table 8. Platinum-catalyzed hydroformylation of styrene.

Entry	Catalyst	Time (h)	Conv. (%)	Yield 40 (%)	Yield 41 (%)
1	<i>trans</i> -[PtCl ₂ (PPh ₃) ₂]	24	40	53	47
2	37	24	55	36	64
3	38	16	60	38	62

Liu and Cui reported on the supramolecular container 42, constructed by using 12 enantiopure Mn(salen)-derived dicarboxylic acids as linear linkers and six Zn₄-*p*-*tert*-butylsulfonylcalix [4] arene clusters as tetravalent four-connected vertices (Figure 7), leading to a chiral octahedral coordination cage that can act as a supramolecular catalyst for the oxidative kinetic resolution (OKR) of racemic alcohols and asymmetric epoxidation of olefins with higher reactivity/enantioselectivity compared with the free metallosalen catalyst [39].

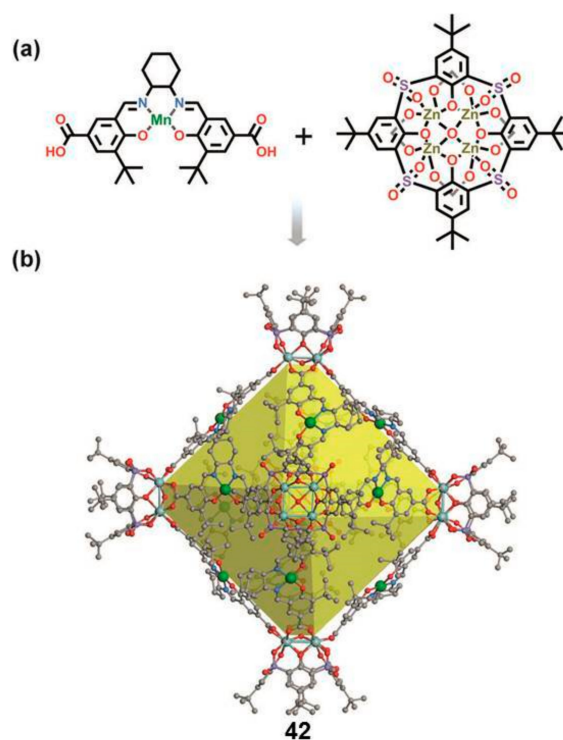


Figure 7. (a) Structures of the building blocks of nanocage 42; (b) single-crystal X-ray structure of the nanocage 42. The cavity is highlighted by a yellow polyhedron (reproduced from Ref. [39], with permission of John Wiley and Sons).

The cage is assembled by the reaction of sulfonylcalix [4] arenes with zinc ions to furnish a shuttlecock-like tetrametallic cluster, which is known to be a four-connected node in making cages, exploiting the coordination with supplementary organic linkers [40].

The authors firstly demonstrated the catalytic activity of the chiral cage in the OKR of racemic secondary alcohols to afford enantiomerically pure secondary alcohols, which are often employed as starting materials for pharmaceutical compounds. All the reactions showed good conversions and excellent enantioselectivities (54–59% conversion and 91–99% of enantiomeric excess) for

1-phenylethanol and its derivatives possessing both electron-withdrawing and electron-donating substituents on the meta/para-position, while ortho-substituted 1-phenylethanol derivatives offered no or low ee values. The resolution of 1-phenylethanol by the chiral supramolecular catalyst afforded the *R* enantiomer in preference to the *S* enantiomer (96% ee), indicating that the enantioselectivity of the reaction is controlled by the handedness of the cage. Furthermore, the catalytic reaction with 1-phenyl-2-propanol, 1-indanol, and their derivatives led to ee values of 86–99.3%. The catalytic activity of the chiral cage was compared with the Mn–Jacobsen catalyst (a well-known catalyst for asymmetric oxidation reactions) for the OKR of 1-indanol, establishing that when the loading was reduced from 0.25 to 0.10 mol %, the chiral cage was still able to afford 60% ee of the product, while the Jacobsen catalyst led to a reaction with no or very little enantioselectivity.

The chiral supramolecular cage was also used as a supramolecular catalyst for epoxidation reactions of 2,2-dimethyl-2H-chromene and its derivatives. All the epoxidation reactions were performed with 0.05 mol % of catalyst with 2-(*tert*-butylsulfonyl) iodosylbenzene (sPhIO) as an oxidant in CH₂Cl₂ at 0 °C, affording the epoxides in 81–96% ee. These results highlight that the cage architecture is able to stabilize the Mn(salen) catalysts, avoid intermolecular deactivation, and encapsulate substrates and reactants in the cavity, increasing reactivity and enantioselectivity.

Cui and coworkers reported on the assembly of five chiral single- and mixed-linker tetrahedral coordination cages (**43–47**, Figure 8) using six enantiopure Mn, Cr, and/or Fe(salen) complexes as linear linkers and four Cp₃Zr₃ clusters as three-connected vertices [41].

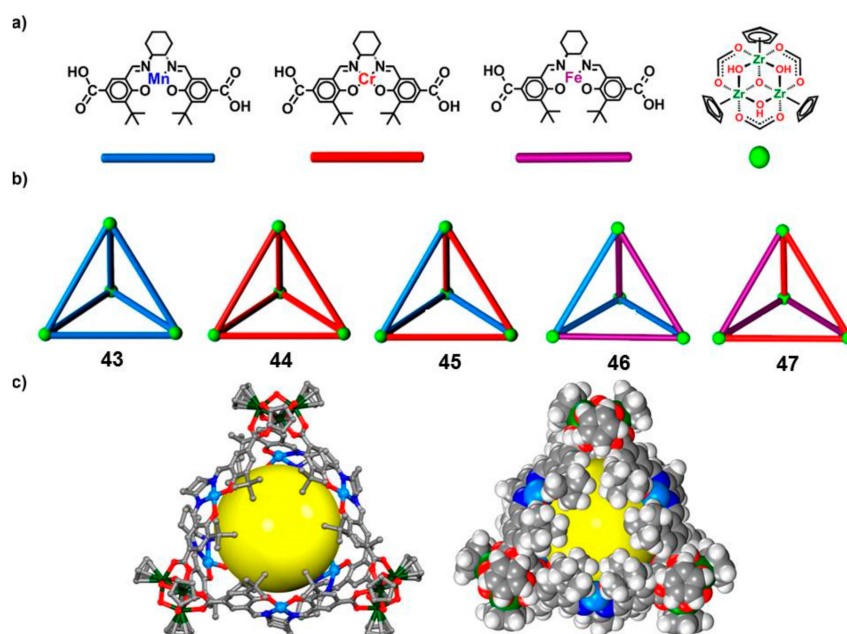


Figure 8. (a) Chemical structures of the metallosalen complexes and trimetallic clusters. (b) Schematic representations of nanocages **43–47**. (c) X-Ray structure and space-filling representation of **43** (adapted with permission from Ref. [41]. Copyright 2008 American Chemical Society).

It is well known that Mn(salen) and Fe(salen) derivatives are excellent catalysts for the enantioselective epoxidation of alkenes [42–46], whereas the Cr(salen) complexes are catalysts for epoxide ring-opening reactions. These supramolecular nanoreactors feature a nanoscale hydrophobic cavity bearing the same or different catalytically active sites. In particular, the cage constructed with Mn(salen) complexes was able to catalyze the asymmetric epoxidation of alkenes, while the cage bearing Cr(salen) complexes catalyzed the ring opening of epoxides. Prompted by these results, the authors assembled a chiral cage bearing both Mn and Cr salen derivatives in which the presence of two different catalytic centers promotes sequential reactions initiated by the epoxidation of alkenes, followed by the ring opening of epoxides. The study of the sequential reaction was initiated with

exposure of 2,2-dimethyl-2H-chromene (DMCH) to PhIO ((diacetoxyiodo) benzene) and a Mn–Cr cage to afford the corresponding epoxide, followed by addition of trimethylsilylazide (TMSN₃) to support the ring opening of the epoxide, providing the azido alcohol in 85% DMCH conversion and 79% yield with 93% ee. Also, DMCH derivatives bearing methyl and nitro groups afforded 78–88% alkene conversions and 73–81% yields with up to 93% ee.

Reek and coworkers reported the first example of the size-selective hydroformylation of alkenes by encapsulation of a rhodium phosphine complex in the molecular cage **48** (Figure 9) [47]. The rhodium complex is strongly bound inside the cavity by a ligand-template approach, due to the presence of pyridyl–zinc (II) porphyrins that led to high association constants (>10⁵ M⁻¹). DFT calculations and in situ high-pressure IR studies of the host–guest complex corroborate the evidence that the encapsulated active species adopt the ee coordination geometry, in which both phosphine ligands are in equatorial positions.

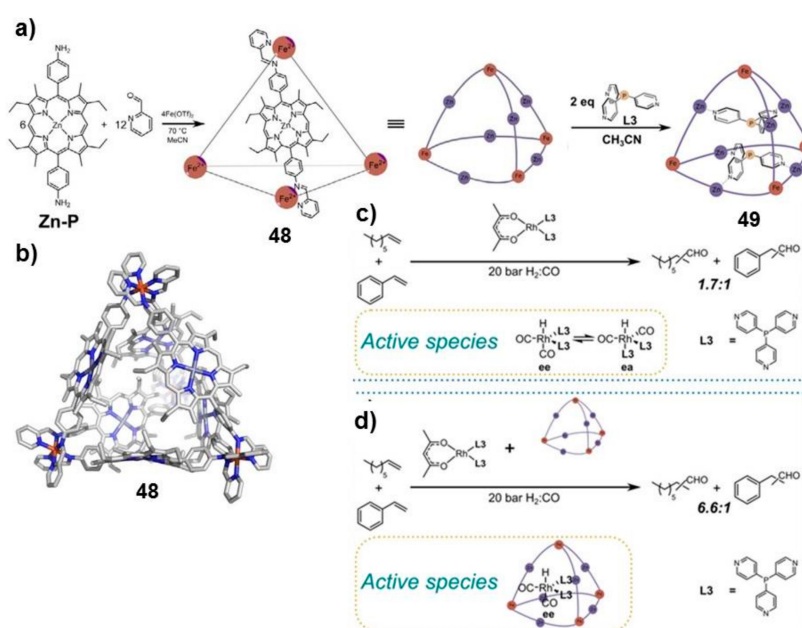


Figure 9. (a) Formation of the tetrahedral cage **48**; (b) optimized structure of cage **48**; (c) formation of the complex between **48** and two trispyridylphosphine ligands, leading to nanocage **49**; (d) hydroformylation of alkenes in solution by a free rhodium phosphine catalyst; (e) hydroformylation of alkenes by an encapsulated rhodium phosphine catalyst into **48** (adapted from Ref. [47], with permission of John Wiley and Sons).

Upon binding of rhodium catalyst, the inner space and the window aperture of the cage slightly decrease, leading to a slower diffusion of larger substrates into the cage compared to that of smaller substrates, which are easily transformed into the corresponding aldehydes. Notably, after activation of the catalyst precursor, followed by the addition of the cage **48**, 1-octene was converted into the corresponding aldehyde with 78% conversion in 72 h at 70 °C, whereas for both selected aromatic guests (styrene and 4-*tert*-butylstyrene), 0% conversion was observed, thus confirming that the encapsulation of rhodium catalyst prevents the access of bulky guests inside the cavity. Furthermore, the authors investigated the reaction of a series of aliphatic alkenes (from 1-hexene to 1-decene; see Figure 10), highlighting that the catalyst preferentially converted shorter substrates.

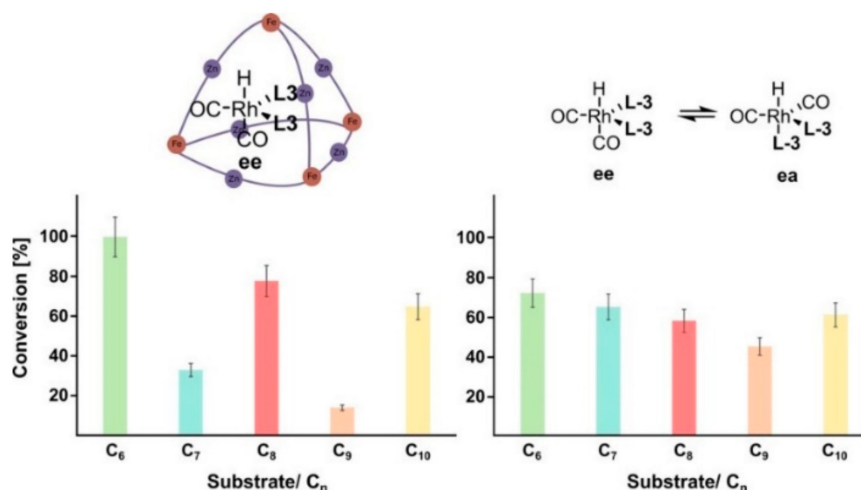


Figure 10. Conversion values obtained in the hydroformylation of alkenes with the nanocatalyst **48** (left) and in the bulk solution (right) (reproduced from Ref. [47], with permission of John Wiley and Sons).

From these data, an odd–even effect is also evident. This particular effect probably depends on an enthalpically more favorable folding of some alkenes inside the cavity. Such an effect is not seen in solution, where the nonencapsulated catalyst transforms all substrates with comparable conversion values.

4. Summary and Outlook

In this review, we have collected the recent progress on catalysis performed inside supramolecular capsules, focusing our attention on hexameric and metallocage capsules. In all cases, the comparison with the analogue reactions in bulk solution shows that reactions in the inner space of these nanoreactors lead to a different reactivity, highlighted by an increase of the rate or by the formation of new product or/and isomers. This feature is similar to those observed in nature: enzymes, in fact, “recognize” the substrate, removing the solvent molecules, thus constraining the reagent in a confined space, increasing the reaction rate, and affording new reaction products. Some common aspects can be found between enzymes and synthetic nanoreactors: (i) regio/stereoselectivity, (ii) stabilization of the transition state, (iii) catalytic properties, and (iv) inhibition by a competitive guest.

In the future, the optimization of geometry, dimension, and affinity for the substrates are the goals in this field. In addition, the catalytic properties of these systems can be exploited in medicine, leading also to theranostic supramolecular nanomaterials [48,49].

Author Contributions: Bibliographic research, R.P.; Writing–Original Draft Preparation, A.P. and G.T.S.; Writing–Review & Editing, G.T.S.

Funding: This research was funded by University of Catania—Department of Chemical Science (Piano per la Ricerca Linea Intervento 2).

Conflicts of Interest: The authors declare no conflict of interest.

References

1. Moran, J.R.; Korbach, S.; Cram, D.J. Cavitands: Synthetic molecular vessels. *J. Am. Chem. Soc.* **1982**, *104*, 5826–5828. [[CrossRef](#)]
2. Cram, D.J. Cavitands: Organic hosts with enforced cavities. *Science* **1983**, *219*, 1177–1183. [[CrossRef](#)] [[PubMed](#)]
3. Heinz, T.; Rudkevich, D.M.; Rebek, J., Jr. Pairwise selection of guests in a cylindrical molecular capsule of nanometre dimensions. *Nature* **1998**, *394*, 764–766. [[CrossRef](#)]

4. Pappalardo, A.; Amato, M.E.; Ballistreri, F.P.; Tomaselli, G.A.; Toscano, R.M.; Trusso Sfrazzetto, G. Pair of Diastereomeric Uranyl Salen CavitanDs Displaying Opposite Enantiodiscrimination of α -Amino Acid Ammonium Salts. *J. Org. Chem.* **2012**, *77*, 7684–7687. [[CrossRef](#)]
5. D'Urso, A.; Tudisco, C.; Ballistreri, F.P.; Condorelli, G.G.; Randazzo, R.; Tomaselli, G.A.; Toscano, R.M.; Trusso Sfrazzetto, G.; Pappalardo, A. Enantioselective extraction mediated by a chiral cavitanD—Salen covalently assembled on a porous silicon surface. *Chem. Commun.* **2014**, *50*, 4993–4996. [[CrossRef](#)] [[PubMed](#)]
6. Ballistreri, F.P.; Brancatelli, G.; Demitri, N.; Geremia, S.; Guldi, D.M.; Melchionna, M.; Pappalardo, A.; Prato, M.; Tomaselli, G.A.; Trusso Sfrazzetto, G. Recognition of C60 by tetra- and tri-quinoxaline cavitanDs. *Supramol. Chem.* **2016**, *28*, 601–607. [[CrossRef](#)]
7. Fujita, M.; Tominaga, M.; Hori, A.; Therrien, B. Coordination assemblies from a Pd(II)-cornered square complex. *Acc. Chem. Res.* **2005**, *38*, 369–378. [[CrossRef](#)] [[PubMed](#)]
8. Gangemi, C.M.A.; Pappalardo, A.; Trusso Sfrazzetto, G. Assembling of Supramolecular Capsules with Resorcin[4]arene and Calix[n]arene Building Blocks. *Curr. Org. Chem.* **2015**, *19*, 2281–2308. [[CrossRef](#)]
9. Pappalardo, A.; Gangemi, C.M.A.; Trusso Sfrazzetto, G. Applications of supramolecular capsules derived from resorcin[4]arenes, calix[n]arenes and metallo-ligands: From biology to catalysis. *RSC Advances* **2015**, *5*, 51919–51933. [[CrossRef](#)]
10. Kubitschke, J.; Javor, S.; Rebek, J. Deep cavitanD vesicles—Multicompartmental hosts. *Chem. Commun.* **2012**, *48*, 9251–9253. [[CrossRef](#)]
11. Weinelt, F.; Schneider, H. Mechanisms of macrocycle genesis. The condensation of resorcinol with aldehydes. *J. Org. Chem.* **1991**, *56*, 5527–5535. [[CrossRef](#)]
12. Ajami, D.; Rebek, J., Jr. Expanding capsules. *Supramol. Chem.* **2009**, *21*, 103–106. [[CrossRef](#)]
13. MacGillivray, L.R.; Atwood, J.L. A chiral spherical molecular assembly held together by 60 hydrogen bonds. *Nature* **1997**, *389*, 469–472. [[CrossRef](#)]
14. Slovak, S.; Avram, L.; Cohen, Y. Encapsulated or not encapsulated? Mapping alcohol sites in hexameric capsules of resorcin[4]arenes in solution by diffusion NMR spectroscopy. *Angew. Chem. Int. Ed.* **2010**, *49*, 428–431. [[CrossRef](#)] [[PubMed](#)]
15. Avram, L.; Cohen, Y. The role of water molecules in a resorcinarene capsule as probed by NMR diffusion measurements. *Org. Lett.* **2002**, *4*, 4365–4368. [[CrossRef](#)]
16. Shivanyuk, A.; Rebek, J., Jr. Reversible encapsulation by self-assembling resorcinarene subunits. *Proc. Natl. Acad. Sci. USA* **2001**, *98*, 7662–7665. [[CrossRef](#)]
17. Avram, L.; Cohen, Y. Discrimination of guests encapsulation in large hexameric molecular capsules in solution: Pyrogallol[4]arene versus resorcin[4]arene capsules. *J. Am. Chem. Soc.* **2003**, *125*, 16180–16181. [[CrossRef](#)]
18. Avram, L.; Cohen, Y.; Rebek, J., Jr. Recent advances in hydrogen-bonded hexameric encapsulation complexes. *Chem. Commun.* **2011**, 5368–5375. [[CrossRef](#)]
19. Gaeta, C.; Talotta, C.; De Rosa, M.; La Manna, P.; Soriente, A.; Neri, P. The Hexameric Resorcinarene Capsule at Work: Supramolecular Catalysis in Confined Spaces. *Chem. Eur. J.* **2019**, *25*, 4899–4913. [[CrossRef](#)]
20. Zhu, Y.; Rebek, J., Jr.; Yu, Y. Cyclizations catalyzed inside a hexameric resorcinarene capsule. *Chem. Commun.* **2019**, *55*, 3573–3577. [[CrossRef](#)]
21. Cavarzan, A.; Reek, J.N.H.; Trentin, F.; Scarso, A.; Strukul, G. Substrate selectivity in the alkyne hydration mediated by NHC–Au(I) controlled by encapsulation of the catalyst within a hydrogen bonded hexameric host. *Catal. Sci. Technol.* **2013**, *3*, 2898–2901. [[CrossRef](#)]
22. La Sorella, G.; Sporni, L.; Strukul, G.; Scarso, A. Supramolecular Encapsulation of Neutral Diazoacetate Esters and Catalyzed 1,3-Dipolar Cycloaddition Reaction by a Self-Assembled Hexameric Capsule. *ChemCatChem* **2015**, *7*, 291–296. [[CrossRef](#)]
23. Giust, S.; La Sorella, G.; Sporni, L.; Strukul, G.; Scarso, A. Substrate selective amide coupling driven by encapsulation of a coupling agent within a self-assembled hexameric capsule. *Chem. Commun.* **2015**, *51*, 1658–1661. [[CrossRef](#)] [[PubMed](#)]
24. Giust, S.; La Sorella, G.; Sporni, L.; Fabris, F.; Strukul, G.; Scarso, A. Supramolecular Catalysis in the Synthesis of Substituted 1HTetrazoles from Isonitriles by a Self-Assembled Hexameric Capsule. *Asian J. Org. Chem.* **2015**, *4*, 217–220. [[CrossRef](#)]

25. La Sorella, G.; Sporni, L.; Strukul, G.; Scarso, A. Supramolecular Activation of Hydrogen Peroxide in the Selective Sulfoxidation of Thioethers by a Self-Assembled Hexameric Capsule. *Adv. Synth. Catal.* **2016**, *358*, 3443–3449. [[CrossRef](#)]
26. Jans, A.C.H.; Gjmez-Suarez, A.; Nolan, S.P.; Reek, J.N.H. A Switchable Gold Catalyst by Encapsulation in a Self-Assembled Cage. *Chem. Eur. J.* **2016**, *22*, 14836–14839. [[CrossRef](#)] [[PubMed](#)]
27. Caneva, T.; Sporni, L.; Strukul, G.; Scarso, A. Efficient epoxide isomerization within a selfassembled hexameric organic capsule. *RSC Adv.* **2016**, *6*, 83505–83509. [[CrossRef](#)]
28. Brauer, T.M.; Zhang, Q.; Tiefenbacher, K. Iminium Catalysis inside a Self-Assembled Supramolecular Capsule: Modulation of Enantiomeric Excess. *Angew. Chem. Int. Ed.* **2016**, *55*, 7698–7701. [[CrossRef](#)] [[PubMed](#)]
29. La Manna, P.; Talotta, C.; Floresta, G.; De Rosa, M.; Soriente, A.; Rescifina, A.; Gaeta, C.; Neri, P. Mild Friedel-Crafts Reactions inside a Hexameric Resorcinarene Capsule: C-Cl Bond Activation through Hydrogen Bonding to Bridging Water Molecules. *Angew. Chem. Int. Ed.* **2018**, *57*, 5423–5428. [[CrossRef](#)]
30. Hofmann, M.; Hampel, N.; Kanzian, T.; Mayr, H. Electrophilic alkylations in neutral aqueous or alcoholic solutions. *Angew. Chem. Int. Ed.* **2004**, *43*, 5402–5405. [[CrossRef](#)]
31. La Manna, P.; De Rosa, M.; Talotta, C.; Gaeta, C.; Soriente, A.; Floresta, G.; Rescifina, A.; Neri, P. The hexameric resorcinarene capsule as an artificial enzyme: Ruling the regio and stereochemistry of a 1,3-dipolar cycloaddition between nitrones and unsaturated aldehydes. *Org. Chem. Front.* **2018**, *5*, 827–837. [[CrossRef](#)]
32. Jacopozzi, P.; Dalcanale, E. Metal-Induced Self-Assembly of Cavitand-Based Cage Molecules. *Angew. Chem. Int. Ed.* **1997**, *36*, 613–615. [[CrossRef](#)]
33. García-Simón, C.; Gramage-Doria, R.; Raoufmoğhaddam, S.; Parella, T.; Costas, M.; Ribas, X.; Reek, J.N.H. Enantioselective Hydroformylation by a Rh-Catalyst Entrapped in a Supramolecular Metallocage. *J. Am. Chem. Soc.* **2015**, *137*, 2680–2687. [[CrossRef](#)] [[PubMed](#)]
34. Dalton, D.M.; Ellis, S.L.; Nichols, E.M.; Mathies, R.M.; Dean Toste, F.; Bergman, R.G.; Raymond, K.N. Supramolecular Ga₄L₆ 12—Cage Photosensitizes 1,3-Rearrangement of Encapsulated Guest via Photoinduced Electron Transfer. *J. Am. Chem. Soc.* **2015**, *137*, 10128–10131. [[CrossRef](#)] [[PubMed](#)]
35. Hong, C.M.; Morimoto, M.; Kapustin, E.A.; Alzakhem, N.; Bergman, R.; Raymond, K.N.; Dean Toste, F. Deconvoluting the Role of Charge in a Supramolecular Catalyst. *J. Am. Chem. Soc.* **2018**, *140*, 6591–6595. [[CrossRef](#)] [[PubMed](#)]
36. Chavagnan, T.; Semeril, D.; Matt, D.; Toupet, L. Cavitand Chemistry—Towards Metallocapsular Catalysts. *Eur. J. Org. Chem.* **2017**, 313–323. [[CrossRef](#)]
37. Amato, M.E.; Ballistreri, F.P.; D'Agata, S.; Pappalardo, A.; Tomaselli, G.A.; Toscano, R.M.; Trusso Sfrazzetto, G. Enantioselective Molecular Recognition of Chiral Organic Ammonium Ions and Amino Acids Using Cavitand-Salen Based Receptors. *Eur. J. Org. Chem.* **2011**, 5674–5680. [[CrossRef](#)]
38. Pappalardo, A.; Amato, M.E.; Ballistreri, F.P.; Notti, A.; Tomaselli, G.A.; Toscano, R.M.; Trusso Sfrazzetto, G. Synthesis and topology of [2 + 2] calix[4]resorcarene-based chiral cavitand-salen macrocycles. *Tetrahedron Lett.* **2012**, *53*, 7150–7153. [[CrossRef](#)]
39. Tan, C.; Jiao, J.; Li, Z.; Liu, Y.; Han, X.; Cui, Y. Design and Assembly of a Chiral Metallosalen-Based Octahedral Coordination Cage for Supramolecular Asymmetric Catalysis. *Angew. Chem. Int. Ed.* **2018**, *57*, 2085–2090. [[CrossRef](#)] [[PubMed](#)]
40. Hang, X.; Liu, B.; Zhu, X.; Wang, S.; Han, H.; Liao, W.; Liu, Y.; Hu, C. Discrete {Ni₄₀} Coordination Cage: A Calixarene-Based Johnson-Type (J17) Hexadecahedron. *J. Am. Chem. Soc.* **2016**, *138*, 2969–2972. [[CrossRef](#)]
41. Jiao, J.; Tan, C.; Li, Z.; Liu, Y.; Han, X.; Cui, Y. Design and Assembly of Chiral Coordination Cages for Asymmetric Sequential Reactions. *J. Am. Chem. Soc.* **2018**, *140*, 2251–2259. [[CrossRef](#)] [[PubMed](#)]
42. La Paglia Fragola, V.; Lupo, F.; Pappalardo, A.; Trusso Sfrazzetto, G.; Toscano, R.M.; Ballistreri, F.P.; Tomaselli, G.A.; Gulino, A. A surface-confined O=MnV(salen) oxene catalyst and high turnover values in asymmetric epoxidation of unfunctionalized olefins. *J. Mater. Chem.* **2012**, *22*, 20561–20565. [[CrossRef](#)]
43. Trusso Sfrazzetto, G.; Millesi, S.; Pappalardo, A.; Toscano, R.M.; Ballistreri, F.P.; Tomaselli, G.A.; Gulino, A. Olefin Epoxidation by a (salen)Mn(III) Catalyst Covalently Grafted on Glass Beads. *Cat. Sci. Techn.* **2015**, *5*, 673–679. [[CrossRef](#)]
44. Ballistreri, F.P.; Gangemi, C.M.A.; Pappalardo, A.; Tomaselli, G.A.; Toscano, R.M.; Trusso Sfrazzetto, G. (Salen)Mn(III) Catalyzed Asymmetric Epoxidation Reactions by Hydrogen Peroxide in Water: A Green Protocol. *Int. J. Mol. Sci.* **2016**, *17*, 1112. [[CrossRef](#)] [[PubMed](#)]

45. Ballistreri, F.P.; Toscano, R.M.; Amato, M.E.; Pappalardo, A.; Gangemi, C.M.A.; Spidalieri, S.; Puglisi, R.; Trusso Sfrazzetto, G. A New Mn–Salen Micellar Nanoreactor for Enantioselective Epoxidation of Alkenes in Water. *Catalysts* **2018**, *8*, 129. [[CrossRef](#)]
46. Zammataro, A.; Gangemi, C.M.A.; Pappalardo, A.; Toscano, R.M.; Puglisi, R.; Nicotra, G.; Fragalà, M.E.; Tuccitto, N.; Trusso Sfrazzetto, G. Covalently functionalized carbon nanoparticles with a chiral Mn–Salen: A new nanocatalyst for enantioselective epoxidation of alkenes. *Chem. Commun.* **2019**, *55*, 5255–5258. [[CrossRef](#)] [[PubMed](#)]
47. Nurttala, S.S.; Brenner, W.; Mosquera, J.; van Vliet, K.M.; Nitschke, J.R.; Reek, J.N.H. Size-Selective Hydroformylation by a Rhodium Catalyst Confined in a Supramolecular Cage. *Chem. Eur. J.* **2019**, *25*, 609–620. [[CrossRef](#)]
48. Yu, G.; Zhao, X.; Zhou, J.; Mao, Z.; Huang, X.; Wang, Z.; Hua, B.; Liu, Y.; Zhang, F.; He, Z.; et al. Supramolecular Polymer-Based Nanomedicine: High Therapeutic Performance and Negligible Long-Term Immunotoxicity. *J. Am. Chem. Soc.* **2018**, *140*, 8005–8019. [[CrossRef](#)]
49. Gangemi, C.M.A.; Puglisi, R.; Pappalardo, A.; Trusso Sfrazzetto, G. Supramolecular complexes for nanomedicine. *Bioorg. Med. Chem. Lett.* **2018**, *28*, 3290–3301. [[CrossRef](#)]



© 2019 by the authors. Licensee MDPI, Basel, Switzerland. This article is an open access article distributed under the terms and conditions of the Creative Commons Attribution (CC BY) license (<http://creativecommons.org/licenses/by/4.0/>).